Assessment of the Safety Factor Evolution of the Shotcrete Lining for Different Curing Ages

Assessment of the safety factor evolution of the shotcrete lining for different curing ages

Pierpaolo Oreste[1], Giovanni Spagnoli[2]*, Cesar Alejandro Luna Ramos[3], Ahmadreza Hedayat[4]

[1] Full Professor, Department of Environmental, Land and Infrastructural Engineering, Politecnico di Torino, Corso Duca Degli Abruzzi 24, 10129 Torino, Italy, pierpaolo.oreste@polito.it, ORCID: 0000-0001-8227-9807

[2] Global Project and Technology Manager Underground Construction, BASF Construction Solutions GmbH, Dr.-Albert-Frank-Straße 32, 83308 Trostberg, Germany, * giovanni.spagnoli@basf.com, ORCID: 0000-0002-1866-4345

[3] Professor, Faculty of Engineering, Universidad Mariana, Faculty of Engineering, Universidad Mariana, Calle 18 No. 34-104, Pasto, Colombia, celuna@umariana.edu.co. Former MSc student at Department of Environmental, Land and Infrastructural Engineering, Politecnico di Torino, Corso Duca Degli Abruzzi 24, 10129 Torino, Italy

[4] Assistant Professor, Department of Civil and Environmental Engineering, Colorado School of Mines, 1500 Illinois Street, Golden, CO 80401, USA, hedayat@mines.edu, ORCID: 0000-0002-7143-7272

Abstract

The behavior of the shotcrete linings during the tunnel construction is complex due to the variability of its mechanical characteristics during the curing time. During the curing time, the lining is loaded along with the excavation face of the tunnel advance. A new calculation procedure involving two analytical methods, i.e. the convergence-confinement method and hyperstatic reaction method have been developed. By means of these two methods, it is possible to assess the evolution of the stress state in the lining, and therefore, also of the safety factor with respect to the failure in compression of the shotcrete. Due to the analysis of the safety factor evolution over time, it is possible to correctly design the lining, to choose the type of sprayed concrete and to define the maximum admissible advance rate of the excavation face, in order not to critically load the lining. In the following paper, after having shown the definition of the safety factor, a parametric analysis is performed, in order to investigate the evolution of the safety factor of the lining for two different rock types, three different shotcrete types and two tunnel advance rates have been considered.

Key words: sprayed concrete; convergence-confinement method; hyperstatic reaction method; accelerator; safety factor; curing age.

No. of Figs: 5

Nomenclature

b	Depth of the lining considered, equal to 1m in the two-dimensional problem taken into consideration
c_{rm} peak	Peak cohesion of the rock mass
c_{rm} res	Residual cohesion of the rock mass
E_{rm}	Elastic modulus of the rock mass
E_{SC}	Elastic modulus of the sprayed concrete with varying time t (in hours) after the lining installation in the studied section
$E_{SC,\infty}$	Asymptotic values of the elastic modulus of the sprayed concrete reached for high time values
FS	Safety factor
$M_{i,j}$	Bending moment in the i-th node, at the load step j-th
$N_{i,j}$	Normal force in the i-th node, at the load step j-th
t	Lining thickness
v	Poisson ratio
α	Exponent of the exponential equation, which characterizes the curing rate, i.e. the evolution of mechanical parameters (elastic modulus and uniaxial compressive strength) of SC over time
ϕ_{rm} peak	Peak friction angle of the rock mass
ϕ_{rm} res	Residual friction angle of the rock mass
ψ	Dilatancy

$\sigma_{n,max,i,j}$ Maximum normal stress acting inside the sprayed concrete in correspondence of a node

σ_{SC} Unconfined compressive strength of the sprayed concrete with varying time t (in hours) after the lining installation in the studied section

$\sigma_{SC,\infty}$ Asymptotic values of the Unconfined compressive strength of the sprayed concrete, reached for high t values

Introduction

DIN 18551 (2014) defines sprayed concrete (or shotcrete), abbreviated here as SC, as "*concrete which is conveyed under pressure through a pneumatic hose or pipe and projected into place at high velocity, with simultaneous compaction*" (see Fig. 1).

Fig. 1 Sprayed concrete trials in a job site.

Because SC takes care of stability problems in tunnels and other underground constructions (Melbye 1994) immediately after the installation, early-age strength and time-dependent behavior of SC both in soil and rock ground conditions is relevant (Thomas 2009); furthermore the time dependent behavior is frequently more important than its ultimate strength, because the advance rate (AR) of the tunnel face is strongly influenced by the rate of development of the SC early-age strength (Mohajerani et al. 2015). The time dependent behavior of shotcrete needs to be considered for realistic ground-support interactions and several constitutive models for shotcrete as a function of curing time currently exist in the literature. Bryne (2014) conducted extensive compressive strength and Young's modulus evaluation of shotcrete with time and developed in-situ test techniques for determination of sprayed shotcrete bond strength. Several studies employed a constitutive law for time dependent stiffness and strength of the shotcrete (e.g., Pan and Huang, 1994; Graziani et al. 2005; Schütz 2010).

The early-age strength of SC is frequently more important than its ultimate strength. The advance speed of tunnel operations is strongly influenced by the rate of development of early-age strength, since it determines, both in soft ground and weak rock, when excavation heading can proceed. As a matter of fact, re-entry is mainly driven by the tunnel drive progression to ensure the safety of personnel to continue development (Mohajerani et al. 2015). Re-entry times range from 2 to 4 h, where the Unconfined Compressive Strength (UCS) reaches 1MPa (Clements 2004; Concrete Institute of Australia 2010), however, this value is not standardized and it can be also lower, if safety is ensured (see Rispin et al. 2009). Iwaki et al. (2001) empirically determined that an UCS of 0.5–1MPa should be an adequate strength for SC to protect against rock-fall, although the safe re-entry times, based on strength measurements, is still determined on project basis (Mohajerani et al. 2015).

Therefore, additives are used to accelerate the hydration reaction (Thomas 2009). Accelerated SC has a shorter final setting time and higher early-age compressive strength compared with conventional concrete (Prudencio 1998) and it can be used in tunneling successfully. The use of accelerators allows for good adhesiveness, lower amount of rebounding, good spraying, and accelerated strength gain, as desired properties for shotcrete (Qiu et al. 2017).

Nowadays, accelerators for SC are normally based on combinations of aluminium salts (sulphates, hydroxides and hydroxysulphates) (DiNoia and Sandberg 2004). Aluminum sulfate is the most common type of accelerator being used (). In wet mix, the accelerator is added in liquid form at the nozzle during spraying. For dry mix, the accelerator can also be added as a fixed dosage in powder form when using pre-bagged mixes (Thomas 2009).

Accelerators considerably improve the setting which should be ≤ 60min (prEN 934-5 2003) for SC applications, against the 6 to 7 h normally needed in Ordinary Portland Cement (De Belie et al. 2005).

In numerical modeling the curing of the cement in the SC lining is very important, as the mechanical improvements (compressive strength and elastic modulus) change the behavior of the linings. These transient conditions are a critical situation for the stability of the support structure during the tunnel construction, influencing the final equilibrium of the lining (Oreste 2003).

There are several methods to numerically model sprayed concrete structures. Elastic method with a constant stiffness (e.g. Pöttler, 1990; Feenstra and de Borst 1993; Rokhar and Zachow, 1997), linear elastic material behavior models (for instance using the Hypothetical Modulus of Elasticity, HME) (e.g. Pöttler 1990), non-linear models considering strain hardening (e.g. Kotsovos and Newman 1978; Aydan et al. 1992; Moussa, 1993; Neville 1995), elastic perfectly plastic constitutive models (e.g. Chen 1982; Hellmich et al. 1999; Thomas 2009), plastic models (e.g. Meschke 1996; Schütz et al. 2011; Schädlich and Schweiger 2014). Nuener et al. (2017) conducted a study and evaluated the influence of different constitutive models for shotcrete on the stresses and displacements in shotcrete shells in deep tunnels and reported different amount of creep and shrinkage in concrete.

The following paper considers the Converge Confinement Method (CCM) and the Hyperstatic Reaction Method (HRM) to jointly study in the detail the behavior of the tunnel support under external loads with different elastic modulus values of SC during the curing phase. The final stress state of the lining is the result of a complex loading mechanism due to the excavation face advance (while the SC hardens) and the corresponding variations in its mechanical characteristics (Oreste 2003). CCM generally requires a mean stiffness of the SC lining to obtain the support reaction line (Oreste 2003). In this research, the reaction line of the SC lining is considered as variable (curved and not linear), in order to simulate the curing effect of the SC during the loading phase of the lining. The variation over time of the elastic modulus of SC is considered by modifying the stiffness of the support and therefore the slope of the reaction line of the SC lining. Time is indirectly considered by associating the different positions of the excavation face with respect to the studied section reached in the time, considering the evolution of the setting time of the SC and therefore to its elastic modulus.

CCM was useful to evaluate the magnitude of the various loading steps developing over time during the face excavation. In HRM method, the interaction between ground and support is represented by Winkler type springs. This method allows for determining the displacement of the lining and the developed bending moments and forces in order to design it (Oreste 2007; Do et al. 2014a). In the specific case, different loading steps obtained with the CCM, have been applied at the HRM model considering for each of these the effective stiffness value reached by the SC and hence by the support structure.

From the calculation results it is possible to determine the final mechanical conditions of the SC lining, that is, when the excavation face is far away from the tunnel section analyzed. Besides, it is also possible to determine, what occurs in the transition phases (for limited timings), when the applied load on the lining is not yet the final one. In this case the SC still has a strength and an elastic modulus lower than the final asymptotic values. From the comparison between the strength reached over the time of the SC and the final stress state in the lining, it is possible to evaluate the safety factor (FS) in the support structure. FS can be plotted as function of time after the installation of the lining in the evaluated section. These graphs are interesting as they allow to evaluate critical situations (minimum FS values) in the transition phases, when SC has not fully cured yet. In this research, after a brief description of the two methods employed for the calculation, a parametric analysis is conducted. The analysis considers three different SC types (with different curing ages) and two difference advancement rates (ARs) of the excavation face (with consequent different load stages of the lining). The analysis allows to assess the evolution of FS over time and to estimate critical phases during the transition load stages of the lining during the SC curing.

The combined analysis of the two calculation methods provided a detailed evaluation of the stress state of the support, which can consider both the effect of the mechanical characteristics of the employed SC (with the evolving curve of strength and stiffness with the time) and the advance rate of the excavation face.

Analytical methods

The analysis of the behavior of the SC linings, during the setting phase and, therefore, during the construction of the tunnel is quite complex with the traditional numerical methods. In fact, it is necessary to update the mechanical characteristics of the SC at each calculation step, linking them with the time after the installation of the lining in the investigated section and the position of the excavation face with respect to the studied section. The knowledge of the evolution of the mechanical parameters of the SC over time, in fact requires to define the elastic modulus of the SC at each calculation step. The position of the excavation face and, therefore, the progress of the excavation work, influences the loading mode of the lining in the studied section. In the three-dimensional numerical methods this happens automatically, since the construction of the tunnel is simulated according to the exact sequence of the excavation steps and the realization of the supports. In two-dimensional numerical methods, however, the position of the face is considered by inserting on the perimeter of the gallery an appropriate fictitious internal pressure, which is gradually decreasing as the excavation face advances.

Given the difficulties of the traditional numerical modeling to represent the correct evolution of the SC during the loading phase of the support, a new calculation procedure was developed (see Oreste et al. 2018a; 2018b) based on two analytical methods, very widespread in the field of tunnels and easy to use: the convergence-confinement method (CCM), see Oreste, (2009; 2014); Fahimifar and Hedayat (2008; 2010) and Spagnoli et al. (2016; 2017) and the hyperstatic reaction method (HRM), see Oreste (2007) and Do et al. (2014a; 2014b). The CCM allows to evaluate with a certain precision the various load steps acting on the lining, and, for each of them, to define the value of the elastic modulus reached by the SC. This is done by determining the convergence-confinement curves of the tunnel and, subsequently, the reaction line of the lining in SC. The latter is determined by points, through the definition of different steps, based on the AR of the excavation face and the evolution of the elastic modulus of the SC over time.

The detailed analysis of the stress state in the lining is then assigned to the HRM. This analytical method uses a numerical solution to finite elements (FEM). The lining is simulated through a succession of one-dimensional elements (beam elements) connected in series through the nodes. On the same nodes of the numerical model, springs (normal and transversal) representing the interaction between the lining and the rock wall of the tunnel are connected. The load steps obtained from the analysis with the CCM are applied to the model and for each of them we proceed to update the elastic modulus of the SC in the one-dimensional elements. The results of the calculation for each load step allow to obtain the progress of the bending moments, of the normal forces and of the shear forces, as well as of the displacements, in the lining, along its whole length. At each load step, the results of that step are then added to the results achieved by all the previous loading steps.

If the bending moment M and the normal force N acting at each node of the lining (i) reached at the load step j are known, it is possible to determine the maximum normal stress $\sigma_{n,max,i,j}$, acting inside the SC in correspondence of that node:

$$\sigma_{n,max,i,j} = \frac{M_{i,j}}{\left(\frac{b \cdot s^2}{6}\right)} + \frac{N_{i,j}}{(b \cdot t)} \quad (1)$$

where:

b: width of the lining considered, equal to 1m in the two-dimensional problem taken into consideration;

$M_{i,j}$: bending moment in the *i-th* node, at the load step *j-th*;

$N_{i,j}$: normal force in the i-th node, at the load step j-th;

t: lining thickness.

Among all the values of $\sigma_{n,max,i,j}$ obtained in the various nodes, the maximum value between the normal stress acting in the various nodes of the model is then identified, which is associated with the j-th load step:

$$\sigma_{n,max,j} = \max(\sigma_{n,max,i,j}) \tag{2}$$

The local safety factor FS_j of the lining on the j-th load step is then evaluated according to the following equation:

$$FS_j = \frac{\sigma_{c,j}}{\sigma_{n,max,j}} \tag{3}$$

where:

$\sigma_{c,j}$: the strength reached by the SC at the j-th load step, knowing the time associated with each load step.

FS calculated above is a local FS, which allows to verify the possible presence of local failure over the SC lining. Local failures do not jeopardize the overall stability of the lining, however they can lead to cracks in the support which may turn out in a global failure. The design of the support must therefore consider local FS values to avoid global failures of the structure.

Since the time t following the realization of the lining in the studied section and the position of the excavation face (in particular the distance reached by the front with respect to the studied section) is associated with each loading step, the calculation procedure allows to plot FS of the SC lining depending on the time or on the distance reached by the excavation face with respect to the studied section. These trends make possible to quickly check whether there is a critical situation in the transient conditions of the lining, or if the minimum FS of the lining is reached in the long term (as an asymptotic value as discussed above). The procedure is able to compare the progress of FS for different types of SC (with and without accelerators) or also for different AR of the excavation face, so that the right type of SC can be chosen to ensure stability both during the construction of the work and in the long term, when the work has been completed.

Results and discussion

To analyze the evolution of FS of the SC lining with the calculation procedure developed, the case of a circular tunnel with 7m radius excavated in two different rock types with RMR = 60 (fair), and RMR = 80 (good), as suggested by Bieniawski (1989), was analyzed. The mechanical characteristics of the two rock masses considered are shown in Tables 1 and 2.

The lithostatic stress state of the rock mass p_0 was assumed to be equal to 7MPa, corresponding to a depth of the tunnel from the ground surface equal to about 300m.

Rock Mass Parameters	Units	Value
Elastic modulus (E_{rm})	[MPa]	21,170
Poisson ratio (v)	[-]	0.30
Peak cohesion (c_{rm} peak)	[MPa]	1.50
Residual cohesion (c_{rm} res)	[MPa]	1.50
Peak friction angle (ϕ_{rm} peak)	[°]	33
Residual friction angle (ϕ_{rm} res)	[°]	33
Dilatancy (ψ)	[°]	16

Table 1. Mechanical characteristics of the rocky type 1 (RMR = 60), considered in the studied example.

Rock Mass Parameters	Units	Value
Elastic modulus (E_{rm})	[MPa]	57,500
Poisson ratio (v)	[-]	0.30
Peak cohesion (c_{rm} peak)	[MPa]	3.75
Residual cohesion (c_{rm} res)	[MPa]	3.75
Peak friction angle (ϕ_{rm} peak)	[°]	42
Residual friction angle (ϕ_{rm} res)	[°]	42
Dilatancy (ψ)	[°]	16

Table 2. Mechanical characteristics of the rocky type 2 (RMR = 80), considered in the studied example.

Pöttler (1990) introduced the coefficient α by suggesting a method to represent the variation of the elastic modulus over the time.

$$E_{,t} = E_{,0} \cdot (1 - e^{-\alpha \cdot t}) \tag{4}$$

where:

- $E_{,t}$ is the SC elastic modulus at the time t;
- $E_{,0}$ is the value of the asymptotic elastic modulus of the SC, for $t = \infty$;

- α is the eexponent of the exponential equation, which characterizes the curing rate, i.e. the evolution of mechanical parameters over time (Oreste 2003).

The ratio between the elastic modulus and UCS is considered constant over time. This is given by the equation of Chang (1993):

$$\sigma_{c,t} = \left(\frac{E_{,t}}{3.86}\right)^{1/0.6} \qquad (5)$$

Where:

$\sigma_{c,t}$ is the UCS for the SC at the time t.

Three different SC types have been considered:

a) a SC with fast curing rate, (SC_A) (α=0.09);

b) a SC with medium curing rate, (SC_B) (α=0.05);

c) a SC with low curing rate, (SC_C) (α=0.03).

For all three SC types, a final value of elastic modulus ($E_{SC,\infty}$=28GPa) and unconfined compressive strength, UCS, ($\sigma_{SC,\infty}$= 27MPa) was arbitrary assumed. The evolution over time of the elastic modulus and UCS was assumed to be identical, that means with the same value of α (Weber 1979; Pöttler 1990; Oreste 2003):

$$E_{SC} = E_{SC,\infty} \cdot (1 - e^{-\alpha t}) \qquad (6)$$

$$\sigma_{SC} = \sigma_{SC,\infty} \cdot (1 - e^{-\alpha t}) \qquad (7)$$

Where:

E_{SC} and σ_{SC}: Elastic modulus and UCS of the SC with varying time t (in hours) after the lining installation in the studied section;

$E_{SC,\infty}$ and $\sigma_{SC,\infty}$: Asymptotic values of the elastic modulus and UCS of the SC, reached for high t values;

The trend over time of the elastic modules and UCS of the SC for the three types considered is shown in Figures 2 and 3.

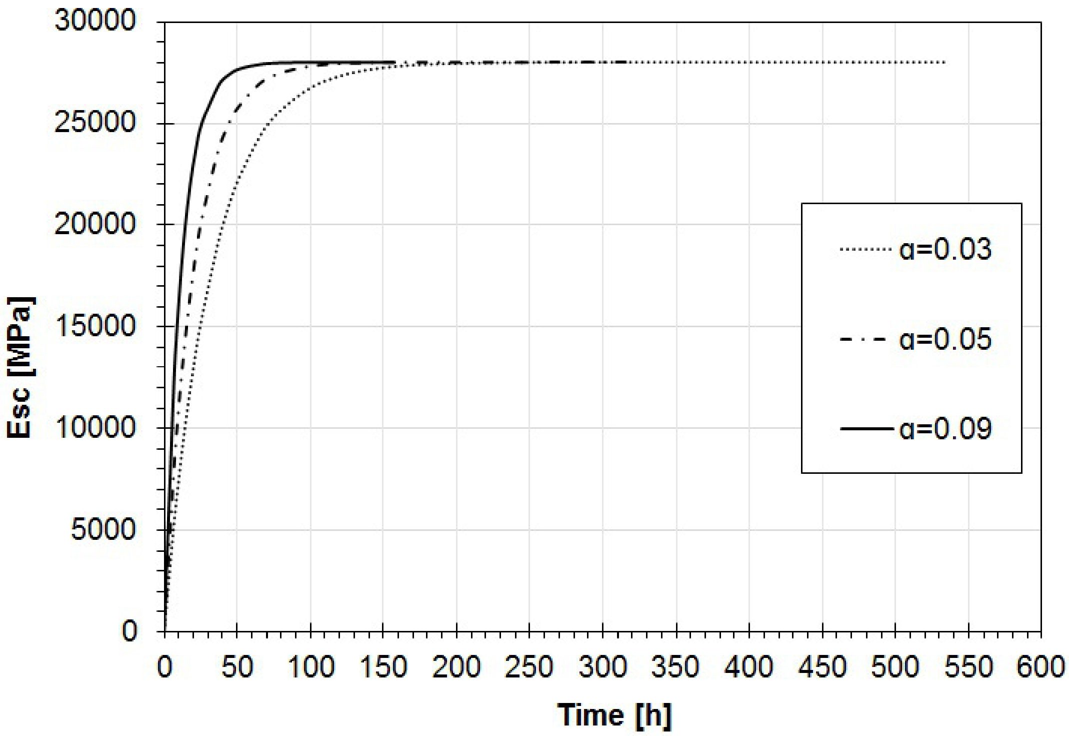

Fig. 2 Trend of the elastic modulus over time for the three SC types considered in the numerical example: SC_A: SC with fast curing rate (α=0.09); SC_B: SC with medium curing rate (α=0.05) and SC_C: SC with low curing rate (α=0.03).

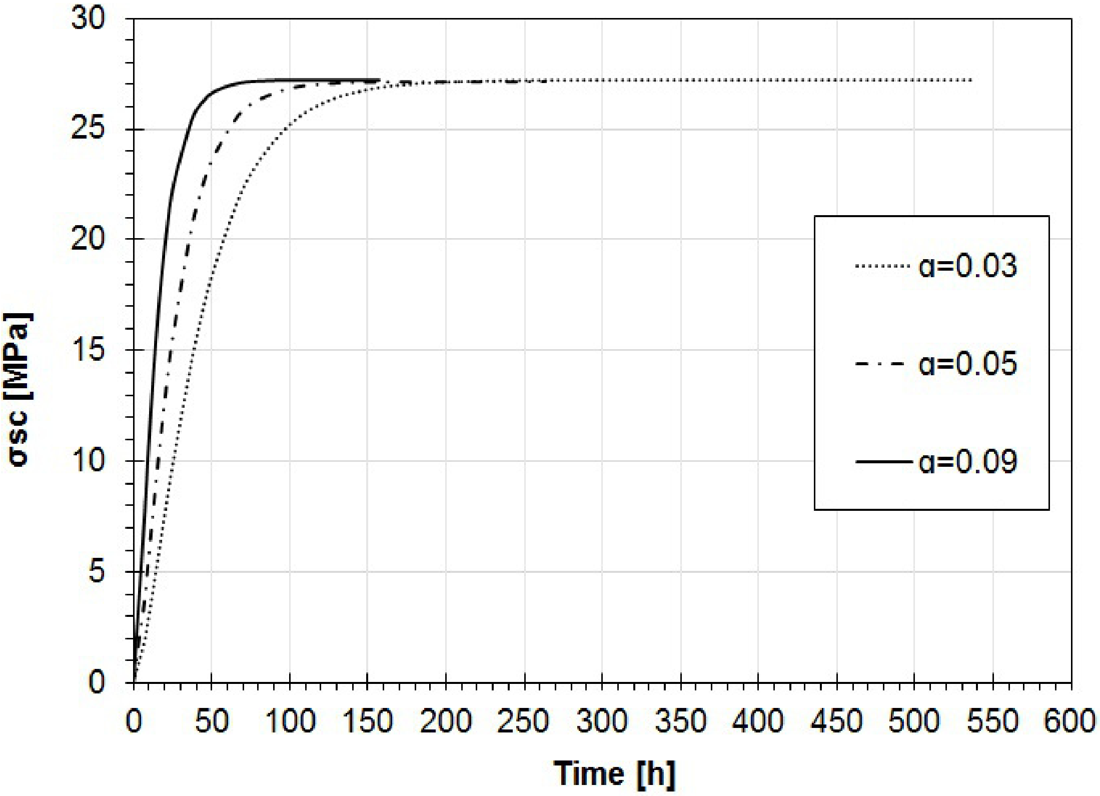

Fig. 3 Trend of UCS over time for the three SC types considered in the numerical example: SC_A: SC with fast curing rate (α=0.09); SC_B: SC with medium curing rate (α=0.05) and SC_C: SC with low curing rate (α=0.03).

Furthermore, two different ARs of the excavation face have been arbitrary considered: 4m/day and 12m/day. The two different rates produce different speed of the load application to the lining, with consequences on the stress state induced in the SC.

The calculation by first the CCM and then with the HRM allowed to determine the values of the bending moments M and of the normal forces N along the development of the entire lining. From the values of M and N the maximum normal stresses in the SC were obtained for each load step and, then, FS with respect to the compression failure. Below the results in terms of FS for the two rock masses, the three types of SC and the two ARs studied are shown. FS are diagrammed according to the time following the lining installation in the studied section.

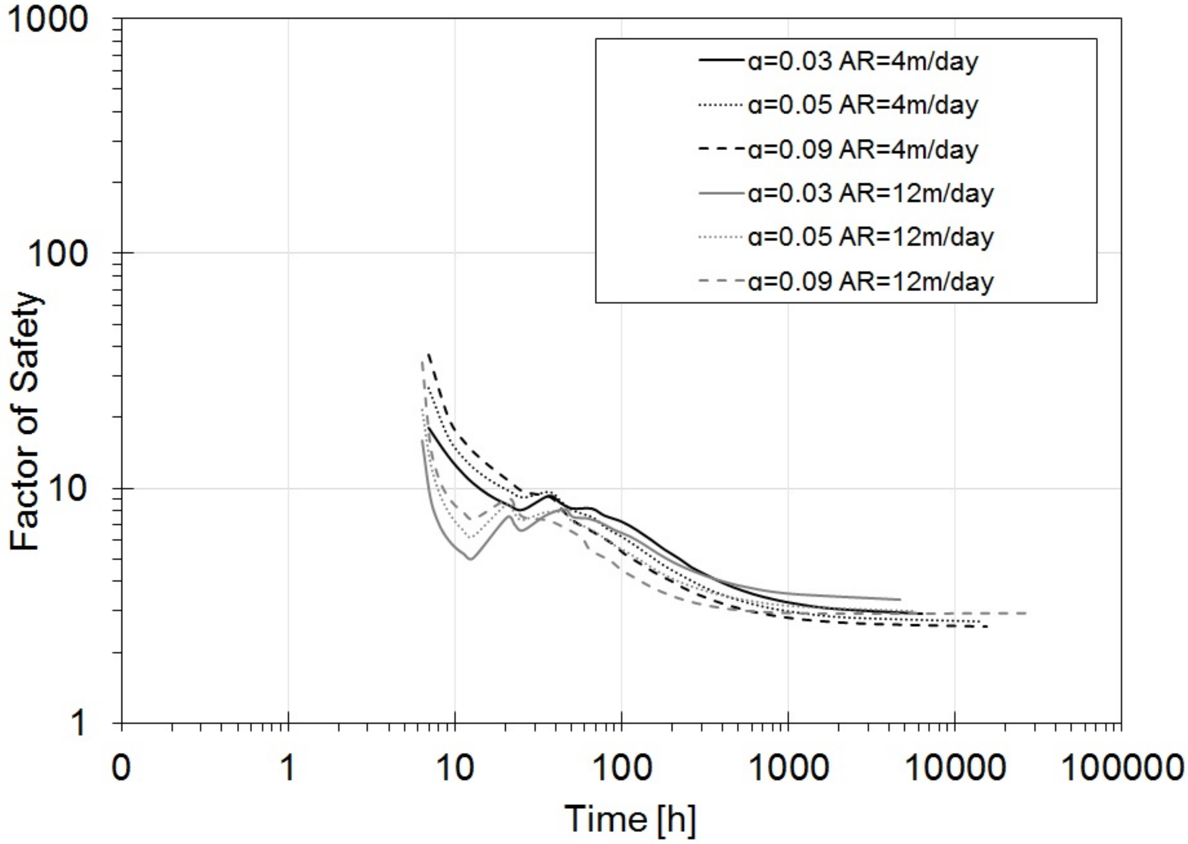

Fig. 4 Rock type 1: Evaluation of FS over time for the three SC types (SC_A (α=0.09), SC_B (α=0.05) and SC_c (α=0.03)) and two advance rates.

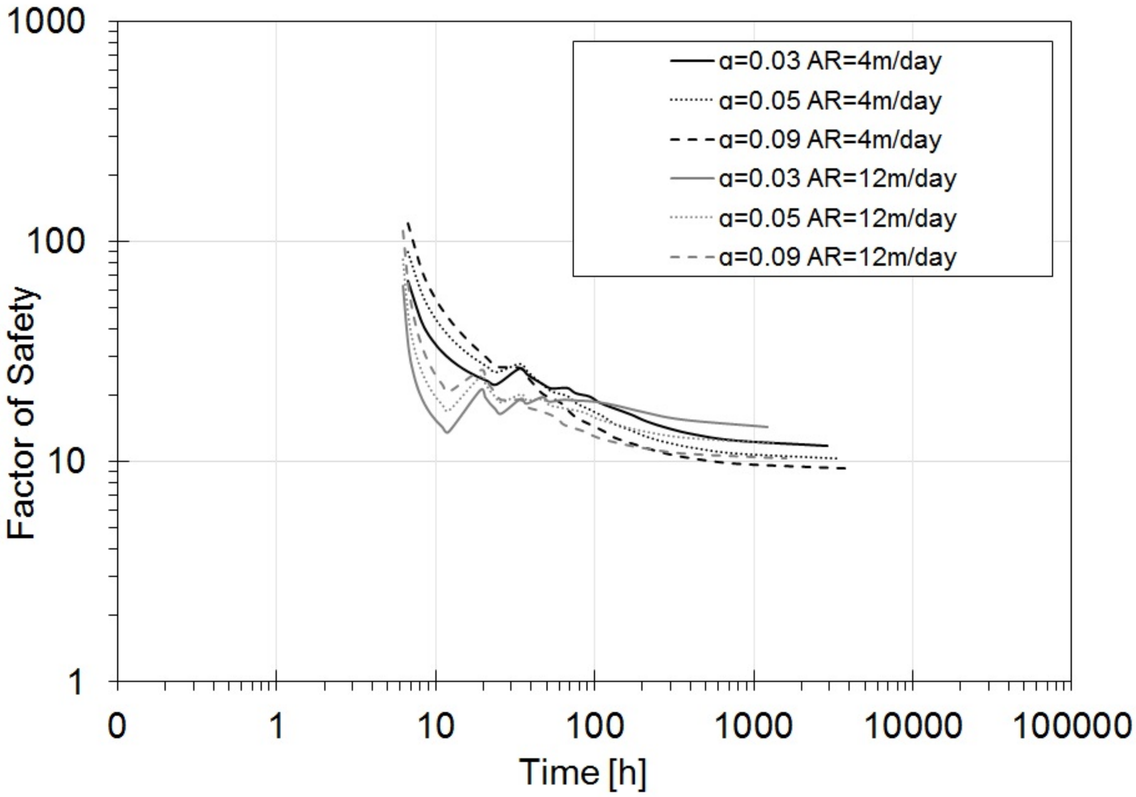

Fig. 5 Rock type 2: Evaluation of FS over time for the three SC types (SC_A (α=0.09), SC_B (α=0.05) and SC_c (α=0.03)) and two advance rates.

The analysis of the results shows above all that the same SC lining has lower **local** FS for the rock type 1, the poorest one among the two considered (Fig. 4). In addition, we note the influence of the type of SC and the AR on FS in both rock masses, mainly for the rock mass with higher geomechanical quality (type 2), see Fig. 5. In general, the long-term FS is lower for fast-curing SCs and lower ARs. AR results to have a negligible effect in the poorest rock mass.

In the transitory conditions, however, there is the presence of relative minima, which may be significant, above all for high ARs and slow curing rate. This phenomenon is more pronounced in the rock mass of superior geomechanical quality. Among the 12 cases studied, just for the case of rock masses type 2, v = 12m/day and type SC_c (with α coefficient of 0.03) a minimum value of FS in the transient condition is noticed (after a few hours compared to the lining installation) lower than the final asymptotic value, representative of the long-term condition.

This circumstance is particularly significant and requires a lot of attention by the tunnel engineers. It can indicate the presence of critical aspects regarding the stability of the lining in a transitory condition, when the SC has not yet completed the curing phase during the tunnel construction.

Conclusions

A new calculation procedure has been used which is able to study in detail the mechanical behavior of the lining during the tunnel construction. This procedure is based on two analytical methods used in succession: the convergence-confinement method (CCM) and the hyperstatic reaction method (HRM). The first one allows evaluating the load steps applied to the lining and, for each one, the value of the elastic modulus reached by the SC. The second helps to calculate the progression of moments, internal forces and displacements, from the results obtained from the first. From the bending moment and the axial force values, it is then possible to determine the safety factor along the perimeter of the lining and the minimum value of the safety factor, representative for the entire support. This safety factor is then plotted over time in order to evaluate the stability conditions of the lining during the tunnel construction.

Subsequently, a parametric analysis was presented analyzing the behavior of the support in two different types of rock mass types, considering two ARs of the excavation face and three types of SC, with different curing rates. The study revealed that, generally, the minimum safety factor is reached in the long term, when the curing of the SC is completed. However, there are circumstances that produce a minimum of the safety factor in the transitory conditions, after a few hours from the lining installation. In these circumstances, the major problems with the stability of the lining are in the short term, rather than in the long term. This can happen above all in the medium-high geomechanical rock types, in the presence of SC with relatively slow curing, with high ARs.

References

1. Aydan, O., Sezaki M. and Kawamoto T. (1992). “Mechanical and numerical modelling of shotcrete,” in Pande, G., Pietruszczack, S. (Eds.), Numerical Models in Geomechanics, Taylor and Francis, London, pp. 707-7016.
2. Bieniawski, Z. T. (1978). "Determining rock mass deformability". Int. J. Rock Mech. Min.Sci., 15, 335–343.
3. Bryne, L. E. (2014). “Time Dependent Material Properties of Shotcrete for Hard Rock Tunneling.” Ph.D Thesis, Stockholm, Sweden.
4. Clements, M. (2004). “Comparison of methods for early age strength testing of sprayed fibre reinforced concrete.” In: Bernard, E.S. (Ed.), Proceedings of the 2nd International Conference on Engineering Developments in Sprayed Fibre Reinforced Concrete, Cairns, Queensland, Australia. Taylor and Francis Group, London, pp. 81–87.
5. Chen, W.F. (1982). Plasticity in Reinforced Concrete. McGraw-Hill, New York.
6. Chang, Y., and Stille, H. (1993). “Influence of early age properties of shotcrete on tunnel construction sequences.” in Wood, D.F., Morgan, D.R. (Eds.), Shotcrete for Underground Support VI, American Society of Civil Engineers, Reston, pp. 110-117.
7. Chang, Y. (1994). “Tunnel support with shotcrete in weak rock- A rock mechanics study.” Ph.D. Thesis, Division of Soil and Rock Mechanics, Royal Institute of Technology, Stockholm, Sweden.
8. Concrete Institute of Australia (2010). Shotcrete in Australia. Concrete Institute of Australia, Rhodes, Australia.
9. De Belie, N., Grosse, C.U., Kurz, J., and Reinhardt, H.W. (2005). “Ultrasound monitoring of the influence of different accelerating admixtures and cement types for

shotcrete on setting and hardening behavior.” Cement Concrete Res., 35, 2087 – 2094.

10. DIN (2014). Spritzbeton - Nationale Anwendungsregeln zur Reihe DIN EN 14487 und Regeln für die Bemessung von Spritzbetonkonstruktionen, Beuth Verlag GmbH, Berlin (in German).
11. DiNoia, T.P., and Sandberg,P.J. (2004). Alkali-free shotcrete accelerator interactions with cement and admixtures. 2nd International Conference on Engineering Developments in Shotcrete, pp. 137-144, A.A. Balkema Publishers , Leiden, London.
12. Do, N.A., Dias, D., Oreste, P., and Djeran-Maigre, I. (2014a). “A new numerical approach to the hyperstatic reaction method for segmental tunnel linings.” Int. J. Numer. Anal. Meth. Geomech., 38,1617–1632.
13. Do, N.A., Dias, D., Oreste, P., and Djeran-Maigre, I., (2014b). “The behavior of the segmental tunnel lining studied by the hyperstatic reaction method.” Eur. J. Environmental Civil Eng. 18(4), 489–510.
14. Fahimifar, A. and Hedayat, A. (2008). “Determination of ground response curve of the supported tunnel considering progressive hardening of shotcrete lining.” Proceedings of the 5th Asian Rock Mechanics Symposium, Tehran, Iran, November 24-26.
15. Fahimifar, A. and Hedayat, A. (2010). “Elasto-plastic analysis in conventional tunnelling excavation.” Proc. Inst. Civ. Eng. Geotech. Eng., 163(1), 37-45, doi: 10.1680/geng.2010.163.1.37.
16. Feenstra, P.H., and de Borst, B. (1993). “Aspects of robust computational models for plain and reinforced concrete,” Heron 48(4), 5-73.
17. Graziani, A., Boldini, D., and Ribacchi, R. (2005). “Practical estimate of deformations and stress relief factors for deep tunnels supported by shotcrete.” Rock Mech. Rock Engng. 38 (5), 345–372.
18. Hellmich, C., Ulm. F.J. and Mang, H.A. (1999). „Multisurface chemoplasticity II: numerical studies on NATM-tunneling.” J Eng. Mech.-ASCE, 125(6): 702-714.

19. Iwaki, K., Hirama, A., Mitani, K., Kaise, S., Nakagawa, K. (2001). „A quality control method for shotcrete strength by pneumatic pin penetration test.” NDT and E International, 34(6), 395-402.
20. Kotsovos, M.D. and Newman, J.B. (1978). “Generalized stress-strain relation for concrete,” J. Eng. Mech.-ASCE,104: 845-856.
21. Melbye, T. (1994). Sprayed Concrete for Rock Support. MBT International Underground Construction Group, Zürich.
22. Meschke, G. (1996). “Elasto-viskoplastische Stoffmodelle fur numeriscbe Simulationen mittels der Methode der Finiten Elemente,“ Habilitationsschrift, TU Wien.
23. Mohajerani, A., Rodrigues, D., Ricciuti, C., and Wilson, C. (2015). Early-Age Strength Measurement of Shotcrete. Journal of Materials, ID 470160, http://dx.doi.org/10.1155/2015/470160.
24. Moussa, A.M. (1993). Finite element modelling of shotcrete in tunnelling. PhD thesis, University of Innsbruck, Austria.
25. Neuner, M., Schreter, M., Unteregger, D., and Hofstetter, G. (2017). “Influence of the Constitutive Model for Shotcrete on the Predicted Structural Behavior of the Shotcrete Shell of a Deep Tunnel.” Materials, 10, 577, doi:10.3390/ma10060577.
26. Neville, A.M., Dilger, W.H., and Brooks, J.J. (1983). Creep of Plain and Structural Concrete. Construction Press, Harlow.
27. Oreste, P. (2003). “Procedure for Determining the Reaction Curve of Shotcrete Lining Considering Transient Conditions.” Rock Mech. Rock Eng., 36(3), 209–236, DOI 10.1007/s00603-002-0043-z.
28. Oreste, P. (2007). “A numerical approach to the hyperstatic reaction method for the dimensioning of tunnel supports.” Tunn. Undergr. Sp. Tech., 22:185–205.
29. Oreste P. (2009). “The Convergence-Confinement Method: Roles and limits in modern geomechanical tunnel design.” American Journal of Applied Sciences 6(4), 757-771.

30. Oreste P. (2014). “The Determination of the tunnel structure loads through the analysis of the Interaction between the void and the support using the convergence-confinement method.”F American Journal of Applied Sciences, 11(11), 1945.1954.
31. Oreste, P., Spagnoli, G., Luna Ramos, C.A., and Sebille, L. (2018). “The Hyperstatic Reaction Method for the Analysis of the Sprayed Concrete Linings Behavior in Tunneling.” Geotech. Geol. Eng., https://doi.org/10.1007/s10706-018-0454-6.
32. Oreste, P., Spagnoli, G., and Luna Ramos, C.A., (2018b). “The Elastic Modulus Variation During the Shotcrete Curing Jointly Investigated by the Convergence-Confinement and the Hyperstatic Reaction Methods.” Geotech. Geol. Eng., https://doi.org/10.1007/s10706-018-0698-1.
33. Pan, Y.W., and Huang, Z.L. (1994). “A model for the time dependent interaction between rock and shotcrete support in a tunnel.” Int. J. Rock Mech. Min. Sci. 31(3), 213-219.
34. Pöttler, R. (1990). “Time-dependent rock—Shotcrete interaction a numerical shortcut.” Comp. Geotech., 9(3), 149-169.
35. prEN 934-5 (2003) Admixtures for Concrete, Mortar and Grout—Part 5: Admixtures for Sprayed Concrete—Definitions, Requirements and Conformity.
36. Prudencio, L.R. Jr (1998). “Accelerating admixture for shotcrete.” Cem. Concr. Compos., 20, 213–219.
37. Qiu, Y., Ding, B., Gan, J., Guo, Z., Zheng, C., Jiang, H. (2017). “Mechanism and preparation of liquid alkali-free liquid setting accelerator for shotcrete”. IOP Conf. Ser. Mater. Sci. Eng., 182, 012034, doi:10.1088/1757-899X/182/1/012034.
38. Rispin, M., Howard, D., Kleven, O. B., Garshol, K., Gelson, J. (2009). “Safer, Deeper, Faster: Sprayed Concrete—An Integral Component of Development Mining,” Australian Centre for Geomechanics.
39. Rokhar, R.B., and Zachow, R. (1997). “Ein neues Verfahren zur taglichen Kontrolle der Auslastung einer Spritzbetonschale,” Felsbau 15(6), 430-434.

40. Schädlich, B. and Schweiger, H.F. (2014). “A new constitutive model for shotcrete,” in: Hicks, M.A., Brinkgreve, R.B.J., Rohe, A. (Eds.), Numerical Methods in Geotechnical Engineering. Taylor & Francis, Oxam, pp. 103-108.
41. Schütz, R. (2010). “Numerical modelling of shotcrete for tunneling” Ph.D Thesis, Imperial College London, UK.
42. Schütz, R., Potts, D.M., and Zdravkovic, L. (2011). “Advanced constitutive modelling of shotcrete: Model formulation and calibration.” Comput. Geotech. 38(6):834–845.
43. Spagnoli, G., Oreste, P., and Lo Bianco, L. (2016). “New Equations for Estimating Radial Loads on Deep Shaft Linings in Weak Rocks.” Int. J. Geomech., 16(6), 06016006, https://doi.org/10.1061/(ASCE)GM.1943-5622.0000657.
44. Spagnoli, G., Oreste, P., and Lo Bianco, L. (2017). “Estimation of Shaft Radial Displacement beyond the Excavation Bottom before Installation of Permanent Lining in Nondilatant Weak Rocks with a Novel Formulation.” Int. J. Geomech., 17(9), 04017051 https://doi.org/10.1061/(ASCE)GM.1943-5622.0000949.
45. Thomas, A. (2009) Sprayed concrete lined tunnels. Taylor & Francis, Oxon.
46. Weber, J. W. (1979). “Empirische Formeln zur Beschreibung der Festigkeitsentwicklung und der Entwicklung des E-moduls von Beton.“ Betonwerk-und-Fertigteiltechnik, 753–759.

Figure caption

Fig. 1 Sprayed concrete trials in a job site.

Fig. 2 Trend of the elastic modulus over time for the three SC types considered in the numerical example: SC_A: SC with fast curing rate (α=0.09); SC_B: SC with medium curing rate (α=0.05) and SC_C: SC with low curing rate (α=0.03).

Fig. 3 Trend of UCS over time for the three SC types considered in the numerical example: SC_A: SC with fast curing rate (α=0.09); SC_B: SC with medium curing rate (α=0.05) and SC_C: SC with low curing rate (α=0.03).

Fig. 4 Rock type 1: Evaluation of FS over time for the three SC types (SC_A (α=0.09), SC_B (α=0.05) and SC_c (α=0.03)) and two advance rates.

Fig. 5 Rock type 2: Evaluation of FS over time for the three SC types (SC_A (α=0.09), SC_B (α=0.05) and SC_c (α=0.03)) and two advance rates.

Table caption

Table 1. Mechanical characteristics of the rock type 1 (RMR = 60), considered in the studied example.

Table 2. Mechanical characteristics of the rock type 2 (RMR = 80), considered in the studied example.